Scripta Materialia 178 (2020) 114–118

Contents lists available at ScienceDirect

Scripta Materialia

journal homepage: www.elsevier.com/locate/scriptamat

Molecular dynamics simulations of ejecta formation in helium-implanted copper

R.M. Flanagan[a,*], E.N. Hahn[a], T.C. Germann[b], M.A. Meyers[a], S.J. Fensin[c]

[a] Department of Mechanical and Aerospace Engineering, University of California San Diego, United States
[b] Theoretical Division, Los Alamos National Laboratory, United States
[c] Materials Science and Technology, Los Alamos National Laboratory, United States

ARTICLE INFO

Article history:
Received 12 August 2019
Revised 29 October 2019
Accepted 2 November 2019

Keywords:
Molecular dynamics
Ejecta
Dynamic behavior

ABSTRACT

The effect of He concentration and morphology on ejecta production is investigated via molecular dynamics simulations. Identical He concentrations are inserted into Cu single crystals as interstitial atoms or bubbles near a flat free surface. The resulting ejecta is quantified through total mass, cluster size, and velocity of ejected particles. The presence of He increases total ejected mass as compared to pure Cu; He bubbles produce 56% more mass than atomic He. This increase is attributed to non-planarities in the shock front and reflected pulse due to He bubbles, akin to ejecta resulting from traditional Richtmeyer–Meshkov instabilities.

When a planar shock wave of sufficient strength encounters a free surface, it is reflected and eventually generates a tensile pulse. In this process, a number of phenomena take place. The best known is spalling, when the reflected pulse reaches a value greater than the tensile strength of the material. Another less known phenomenon is the ejection of matter from the free surface, producing what is known as ejecta. The formation of ejecta was explored by Asay and associates in the 1970s [1–3] and is a special case of the Richtmeyer-Meshkov Instability (RMI) [4–6]. RMI occurs when the shock front interacts with a roughened surface, causing the peaks and valleys of the surface to invert when impacted, forming finger-like jets that grow and may eventually break-up into smaller clusters of atoms. Previous work reveals that the mass of total ejecta produced is proportional to the surface roughness [2–4], and measurements of particle size distributions show a power-law scaling, in agreement with percolation theory [7–9]. Theoretical and experimental studies on crystalline metals have explored the role of surface roughness, particle velocity, and crystalline phases but have historically neglected material microstructure. This can mostly be attributed to the fact that total ejected mass significantly increases once the material melts while a negligible mass is usually produced in the solid state [1]. Few studies mention the importance of heterogeneities such as voids or inclusions to ejecta production, but even those that do mainly focus on the role of surface roughness and particle velocity [1,8,10,11]. As materials are developed for use in extreme environments, where heterogeneities are formed through sustained damage, understanding the role of microstructure in dynamic behavior and strength is crucial.

Damage can form through countless processes such as irradiation, which is known to produce vacancies, voids, and dislocations which lead to a degradation in the material properties [12–14]. Helium atoms can also be present in the microstructure, mostly through radioactive decay, and can eventually coalesce into bubbles due to the low solubility of helium in metals, including copper [15,16]. The presence of helium in crystalline materials has been shown to cause embrittlement [14,17], swelling [12,14,18–20], and hardening. The dynamic behavior, including ejecta production, of helium-implanted materials has become of great interest [9,21–24] since it has been shown that presence of helium may play an important role in material strength [24].

This work investigates the effect of helium concentration and its morphology on ejecta production from single crystal ⟨111⟩ copper using molecular dynamics (MD) simulations. This simulation technique not only allowed us to tailor the concentration and morphology of the helium in a systematic manner but also provided time-resolved data to understand the appropriate mechanisms underlying ejecta production. It is important to note that due to differences in both length and time scales between molecular dynamics and experiments, it is inappropriate to quantitatively compare data from these simulations to experimental observations; rather, the trends in the data should stay consistent. The simulations described in this work provide insight into if and why heterogeneities

* Corresponding author.
E-mail addresses: rflanaga@eng.ucsd.edu, rmf@lanl.gov (R.M. Flanagan).

https://doi.org/10.1016/j.scriptamat.2019.11.005

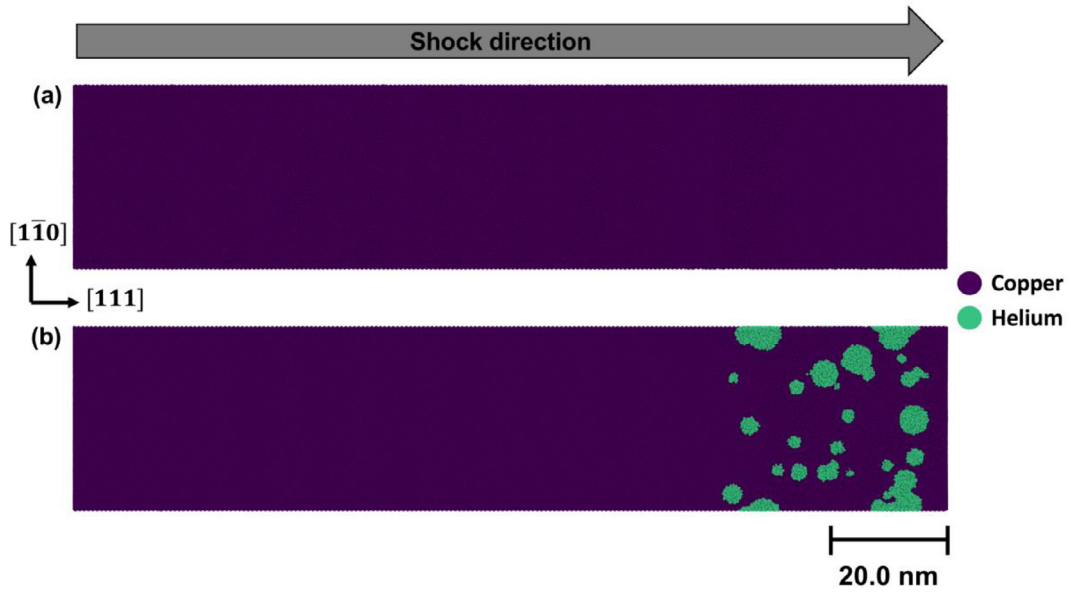

Fig. 1. Initial configuration of piston shock simulations. (a) Perfect FCC single crystal copper and (b) FCC single crystal implanted with helium bubbles are piston-shocked along the [111] direction. The helium bubbles are randomly distributed throughout the end of the sample with an average radius of 1 nm with 1 helium atom per copper vacancy.

are important for ejecta production but not for absolute quantitative data. Experiments are currently underway to validate trends observed in these simulations.

Simulations were performed using a splined EAM potential from Kashinath and Demkowicz [25] to model interactions between all atoms, which was implemented into the Scalable Parallel Short-range Molecular dynamics (SPaSM) code [26]. Results were analyzed using Ovito [27]. To solely focus on the effects of helium concentration and morphology, a simulation cell of single crystal copper oriented such that the [11$\bar{2}$], [1$\bar{1}$0], and [111] crystallographic directions align along the x, y, and z axes respectively. All simulation cells had dimensions of $60 \times 60 \times 300$ units lattice (1 unit lattice is 0.3615 nm), totaling 6.4 million atoms, and all surfaces were flat. This configuration allowed us to separate the effect of helium from machined perturbations on ejecta production. To alter the concentration and morphology of the He bubbles, four configurations of monocrystalline copper were investigated: 1) no added helium, 2) 1.5 vol% interstitial helium, 3) 1.5 vol% helium bubbles, and 4) 1.5 vol% voids. Helium defects can reach up to 8% concentration in metals [28] but defect concentrations of 5% or greater have been shown to alter the equation of state measurably [29], so the He concentration is limited to 1.5% atomic concentration. For cases 2–4, the defects were randomly implanted within a region 33 nm from the free surface. The ratio of the region containing defects to the region containing pure Cu is proportional to helium-implanted metals studied experimentally (<10%) [28]. For helium bubbles and voids, a random seed was used to achieve an average radius of 1 nm. Additionally, to control the pressure within the bubbles, a 1–1 Cu-He substitution was performed. Examples of the initial configurations are shown in Fig. 1.

Each simulation was equilibrated with a Nosé-Hoover isobaric-isothermal ensemble (NPT) at 0 pressure and 300 K for 50 ps. The system was then shocked along the <111> direction using a momentum mirror [30] at a specified particle velocity. This orientation was selected for comparison to previously existing simulation data for pure, flat copper [9]. The particle velocity ranged from 2.0 to 4.5 km/s. The simulation cell is periodic in the x and y dimensions and a large vacuum region is added along the shock direction to allow for transport of ejecta atoms. A virtual boundary is placed downstream of the free surface at a distance equal to the initial length of the simulation cell in the shock direction. All copper atoms that cross this boundary are counted as ejecta. The number of copper atoms passing through the boundary linearly increases in time until the free surface reaches the boundary, at which point the static boundary technique is no longer appropriate for evaluating ejected quantities. The number of ejected atoms is converted to ejected mass using the molar mass of copper; the areal density is the quotient of the ejected mass and the cross-sectional area of the simulation perpendicular to the shock direction. Only copper atoms are counted as ejected mass since diagnostics such as lithium niobite pins used to measure mass in RMI experiments are unable to measure helium due to its low atomic mass. Cluster analysis was performed using OVITO [28] with a cutoff of 0.2825 nm.

Fig. 2 shows the total ejected mass as a function of particle velocity. Resulting areal density for pure copper in this work agrees with previous results of Germann et al. [9], where the sharp rise in total ejected mass is linked to shock melting of copper. However, increasing the concentration of atomic helium located within the Cu lattice from 0 to 1.5 vol% triples the ejecta production when the material is still in solid state. This solid ejected mass is altered further as a function of morphology while the concentration is held constant. Specifically, addition of 1.5 vol% helium bubbles increases the total ejected mass by 2 orders of magnitude in comparison to pure copper. This was surprising because it is well accepted from previous results [1] that negligible ejecta mass is produced when a material is in solid state. The observed increase in total ejected mass as a function of helium concentration also occurs upon shock melting of copper. The origin for significant changes in ejected mass seen in this study are attributed to either an alteration of the equation of state or of the morphology of the shock front.

To investigate the equation of state as a function of helium concentration and morphology, additional simulations with the Hugoniostat method [31] in LAMMPS [32] were performed using the same Cu-He interatomic potential. The Hugoniostat method is an equilibrium molecular dynamics formulation which manipulates heat flow and uniaxial strain rate to compress a material along the specified shock direction, satisfying conservation of mass, momentum, and energy throughout the system [31]. This method allows for a computationally efficient calculation of a material's equation

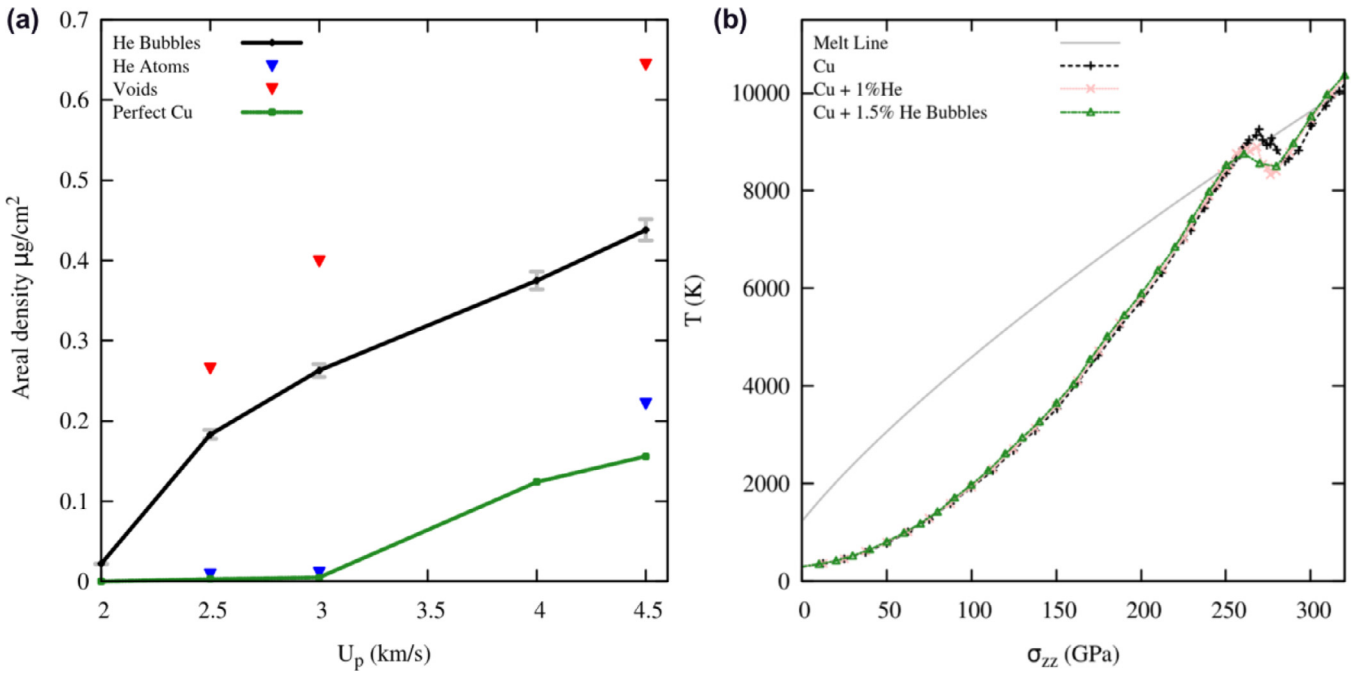

Fig. 2. (a) Areal mass density of ejecta from Cu simulations performed at an initial temperature of 300 K along the <111> direction. The pure Cu case is in agreement with the pure Cu case from Germann, et al. while the helium and void implanted cases show an increase in ejecta. (b) The relationship between shock pressure and temperature in comparison to the pure Cu PT curve reveals that low concentrations of helium decrease the shock melt by 8% or less.

of state during shock. Simulations performed in this study used a cell of $40 \times 23 \times 32$ units lattice consisting of 703,991 atoms. To isolate the effect of concentration from morphology, three types of single crystal copper were modeled: 1) pure copper, 2) copper seeded with 1% volume of helium in substitutional sites, 3) and copper implanted with 1.5% bubbles, with an average radius of 1 nm. All defects were randomly dispersed throughout the material, not just on the surface. The results from these calculations show that there is less than a 7.8% decrease change in the shock melting point for copper implanted with helium bubbles and 5.6% decrease in that of copper implanted with atomic helium as compared to pure copper, shown in the inset of Fig. 2. These results are consistent with other studies, which show that a large percentage of defects (5% or more) are needed to alter the equation of state of a material in a measurable manner [25].

Since ejecta production is traditionally associated with the RMI phenomenon, occurring when a shock front interacts with a roughened surface, it was also hypothesized that in the case of copper with a flat surface, heterogeneities can act as sources that can cause the shock front to become non-planar, thus leading to an increase in ejected mass. This would be akin to having the machine "perturbations" underneath the free surface rather than *on* the free surface. Hence, even with a flat surface, some ejected mass production is expected. To test the validity of this hypothesis as the cause for our observations of increased ejected mass as a function of He concentration and morphology, additional analysis on the simulations at a particle velocity of 4.5 km/s, where copper is melted.

While pure copper and copper with atomic helium produced a small amount of mainly atomic ejecta, copper with helium bubbles produced "finger-like" ejecta whose morphology appeared to be characteristic of RMI-induced ejecta despite the initial free surface being flat. This seems to be consistent with the development of a non-planar shock front due to the presence of helium bubbles. To further understand the importance of helium bubbles, simulations using empty voids rather than helium bubbles were performed. Ejecta production from copper with voids not only produced the highest total mass but also led to the formation of a chaotic "finger" like ejecta formation qualitatively similar to copper with helium bubbles. The formation of ejecta in this work is related to the fact that the helium bubbles, due to differences in shock impedance as compared to the rest of the material, alter the shock velocity in their local vicinity. This causes a non-planarity to develop in the shock front because of changes in the shock velocity in the neighborhood of the helium bubbles. These "ripples" in the shock front reach the free surface and create an effect similar to the material having a rough surface. This is highlighted in the attached figure where variations in the position of the atoms are shown due to the non-planar morphology of the shock front. In addition to this variability, the shock wave compresses the bubbles, causing internal jetting similar to a shape-charge like phenomenon [20]. These internal jets further contribute to ejected mass from the surface. The formation of small jets suggests that the presence of any heterogeneity with a lower/higher density, compared to the parent metal matrix, leads to the creation of a non-planarity in the shock front whose magnitude is proportional to the difference in density and size of the heterogeneity.

The effect of this density difference on the morphology of the shock front in all four cases is shown in Fig. 3a. The differences in velocities of the shock front, especially due t helium bubbles and voids, indeed show the formation of larger non-planarities in the shock front as compared to the copper with atomic helium. The local increase in velocity due to bubbles and voids is associated with the collapse of these heterogeneities which not only contributes pressure-volume work in the form of an increase in kinetic energy to the system [33] but also forms internal jets similar to shaped charges, as observed in Fig. 3a. This internal jetting of material alters the morphology of ejecta produced from the surface of copper, shown in Fig. 3b. This is also quantitatively observed in the cluster size analysis shown in Fig. 4.

The copper with helium bubbles shows an order-of-magnitude increase in ejecta cluster sizes compared to pure copper; the largest cluster has 500 atoms in comparison with 10 atoms. This is consistent with the qualitative results shown in Fig. 3b. Additionally, the velocity of the larger clusters tends towards the free

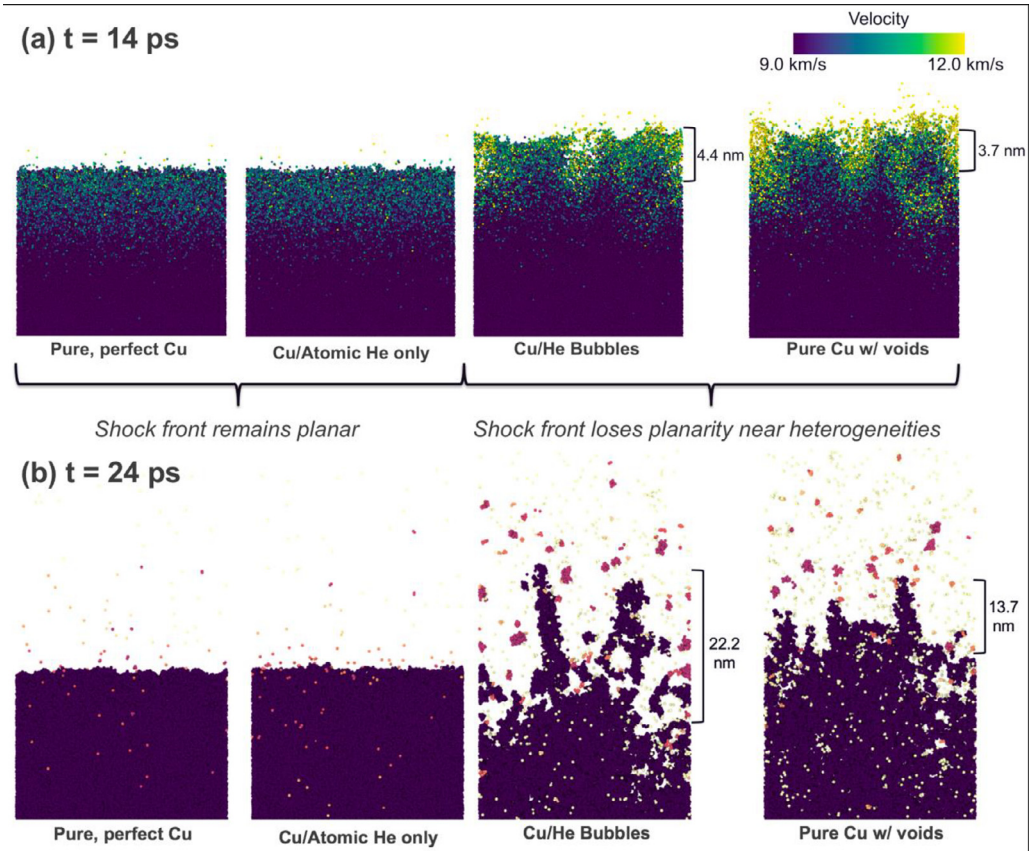

Fig. 3. (a) At a particle of 4.5 km/s, the nonplanar shock front interacts with the free surface, leading to immediate jetting on the order of several nanometers and increased velocity due to the added kinetic energy from bubble collapse. (b) 10 ps later, the ejecta for the pure and atomic helium cases is quite small while the bubble and voids cases develop large clusters and finger-like jets, which are characteristic of traditional RMI studies.

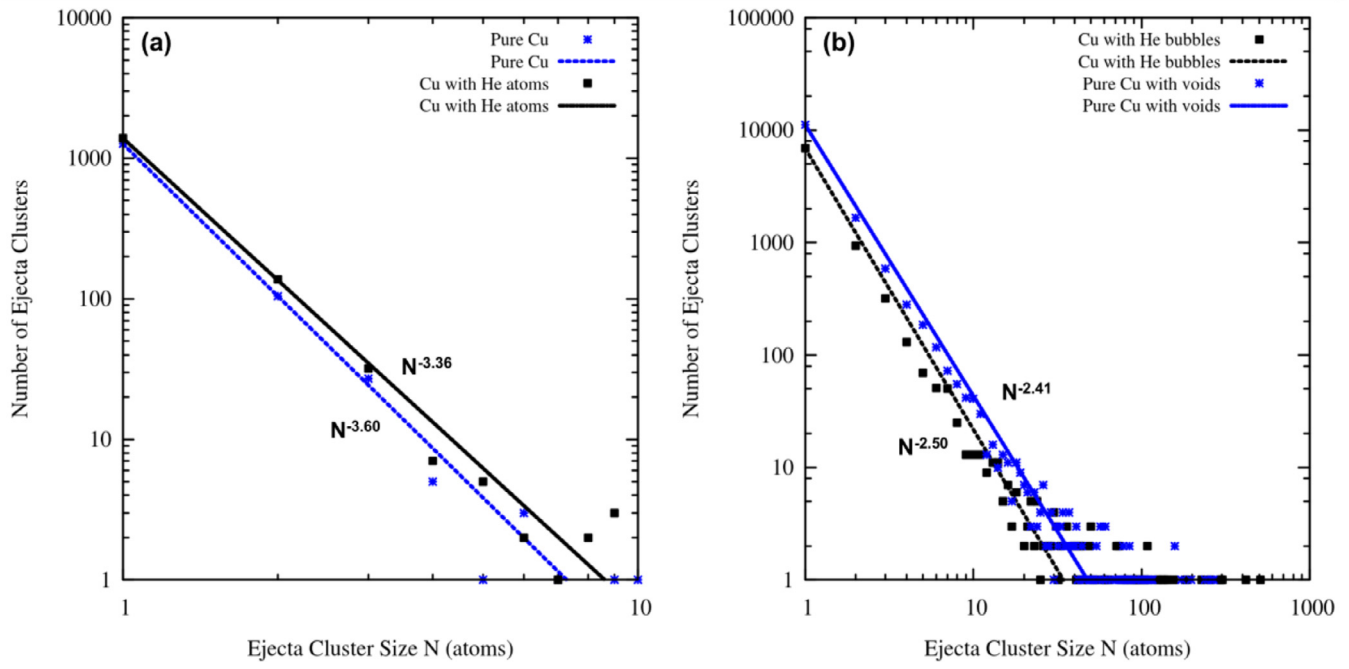

Fig. 4. Distribution of ejecta particle sizes for <111> Cu crystals shocked with $u_p = 4.5$ km/s. (a) Cu implanted with interstitial He produces slightly more ejecta than for the pure Cu case, although the cluster sizes are similar. (b) Single crystal Cu with voids at the surface produces more ejecta than Cu implanted with He bubbles, but the bubbles produce the largest clusters.

surface velocity of the material, although the free surface velocity measured in pure copper (9.825 km/s) is noticeably lower than in copper with helium bubbles (10.38 km/s) despite having the same initial particle velocity. This is due to the collapse of bubbles, which does plastic work and imparts extra energy to the free surface atoms. This difference in cluster size and velocity has implications to the long-term evolution of ejecta, a topic that is not discussed in the present study.

To further highlight the differences in ejecta production, the total ejecta is subdivided into two specific categories: monoatomic and multi-atomic. Our results show that monoatomic ejecta in pure copper has an average velocity of 10.6 +/- 0.89 km/s while monoatomic ejecta in copper with helium bubbles have an average velocity of 11.2 +/- 1.22 km/s. While the standard deviations of these cases intersect, the increased mean and spread of the velocities in the latter case supports the idea that the kinetic energy of these surface atoms increases as a result of pressure-volume work done by bubble collapse during shock. Further analysis of the number and size of ejecta clusters, shown in Fig. 4, highlights the difference in cluster sizes and their number as a function of helium concentration and morphology. The configuration of helium bubbles has a larger impact on the size of clusters generated as mentioned above. Using a power law fit, percolation theory is used to understand the difference in this behavior. Percolation theory explains the tendency of objects to cluster with a power law fit whose exponent indicates the dimensionality or other physical mechanisms of clustering. In the present work, the difference in exponents of the power law as a function of helium morphology from 2.4 to 3.4 (as shown in Fig. 4a and b) again suggests that the addition of helium alters the mechanisms involved in ejecta production. These results agree with results of Werdiger et al., who also suggest that different mechanisms of ejecta production are related to different ejecta morphology. For example, hydrodynamic instabilities are related to the jet-like structure in Sn ejecta while microspalling contributes to the cloud-like ejecta observed in Al [7]. In conclusion, our work shows a profound effect of heterogeneities on ejecta production and is a step in the right direction to eventually understand and accurately predict ejected masses.

Acknowledgements

Molecular dynamics simulations utilized resources were provided by the LANL Institutional Computing Program and funding was provided by the Science Campaigns. The support provided to Rachel Flanagan and Marc Meyers by the Center for Matter in Extreme Conditions (award number DE-NA0003842) is gratefully acknowledged. This work was supported by the U.S. Department of Energy (DOE) through the Los Alamos National Laboratory. The Los Alamos National Laboratory is operated by Triad National Security, LLC, for the National Nuclear Security Administration of the U.S. Department of Energy (Contract No. 89233218CNA000001).

References

[1] J.R. Asay, Material ejection from shock-loaded free surfaces of aluminum and lead, SAND-76-0542, 7136578, Oct. 1976.
[2] J.R. Asay, L.D. Bertholf, Sandia Lab. (1978) Oct.
[3] J.R. Asay, L.P. Mix, F.C. Perry, Appl. Phys. Lett. 29 (5) (1976) 284–287.
[4] E.E. Meshkov, Fluid Dyn. 4 (5) (1969) 101–104.
[5] R.D. Richtmyer, Commun. Pure Appl. Math. 13 (2) (1960) 297–319.
[6] K.A. Meyer, P.J. Blewett, Phys. Fluids 15 (5) (1972) 753–759.
[7] M. Werdiger, et al., Laser Part Beams 14 (02) (1996) 133.
[8] D.S. Sorenson, R.W. Minich, J.L. Romero, T.W. Tunnell, R.M. Malone, J. Appl. Phys. 92 (10) (2002) 5830–5836.
[9] T.C. Germann, et al., AIP Conf. Proc. 706 (1) (2004) 285–288.
[10] P. Andriot, P. Chapron, F. Olive, AIP Conf. Proc. 78 (1) (1982) 505–509.
[11] V.A. Ogorodnikov, A.G. Ivanov, A.L. Mikhailov, N.I. Kryukov, A.P. Tolochko, V.A. Golubev, Combust. Explos. Shock Waves 34 (6) (1998) 696–700.
[12] H. Trinkaus, B.N. Singh, J. Nucl. Mater. 323 (2–3) (2003) 229–242.
[13] T. Yamamoto, G.R. Odette, P. Miao, D.J. Edwards, R.J. Kurtz, J. Nucl. Mater. 386–388 (Apr. 2009) 338–341.
[14] R.S. Barnes, G.B. Redding, A.H. Cottrbll, Philos. Mag. 3 (25) (1958) 97–99.
[15] P.A. Thorsen, J.B. Bilde-Sørensen, B.N. Singh, Scr. Mater. 51 (6) (2004) 557–560.
[16] R.S. Barnes, Nature 206 (1965) 1307–1310.
[17] V. Raineri, S. Coffa, E. Szilágyi, J. Gyulai, E. Rimini, Phys. Rev. B 61 (2) (2000) 937–945.
[18] D.F. Cowgill, Fusion Sci. Technol. 48 (1) (2005) 539–544.
[19] L. Pizzagalli, M.L. David, M. Bertolus, Model. Simul. Mater. Sci. Eng. 21 (6) (2013) 065002.
[20] B. Li, L. Wang, J.C. E, H.H. Ma, S.N. Luo, J. Appl. Phys. 116 (21) (2014) 213506.
[21] Q. Guo, P. Landau, P. Hosemann, Y. Wang, J.R. Greer, Small 9 (5) (2013) 691–696.
[22] B. Glam, M. Strauss, S. Eliezer, D. Moreno, Int. J. Impact Eng. 65 (2014) 1–12.
[23] H.-Y. Wang, X.-S. Li, W.-J. Zhu, X.-L. Deng, Z.-F. Song, X.-R. Chen, Radiat. Eff. Defects Solids 169 (2) (2014) 109–116.
[24] M.B. Prime, et al., J. Phys. Conf. Ser. 500 (11) (2014) 112051.
[25] A. Kashinath, M.J. Demkowicz, Model. Simul. Mater. Sci. Eng. 19 (3) (2011) 035007.
[26] D.M. Beazley, P.S. Lomdahl, Parallel Compu.t 20 (2) (1994) 173–195.
[27] L.A. Zepeda-Ruiz, A. Stukowski, T. Oppelstrup, V.V. Bulatov, Nature 550 (7677) (2017) 492–495.
[28] N. Li, M.J. Demkowicz, N.A. Mara, JOM 69 (11) (2017) 2206–2213.
[29] E.N. Hahn, S.J. Fensin, J. Appl. Phys. 125 (21) (2019) 215902.
[30] W. Han, et al., J. Mater. Res. 28 (20) (2013) 2763–2770.
[31] B.L. Holian, Science 280 (5372) (1998) 2085–2088.
[32] R. Ravelo, B.L. Holian, T.C. Germann, P.S. Lomdahl, Phys. Rev. B 70 (1) (Jul. 2004) 014103.
[33] S. Plimpton, J. Comput. Phys. 117 (1) (1995) 1–19.